Polym. Korea, Vol. 47, No. 4, pp. 427-439 (2023)
https://doi.org/10.7317/pk.2023.47.4.427

ISSN 0379-153X(Print)
ISSN 2234-8077(Online)

나노그래핀 산화물 첨가에 따른 EPDM/SBR 나노복합소재의 기계적 물성 연구

P. C. Prakash†, G. Gurumoorthi, V. Navaneethakrishnan, and S. Vishvanathperumal*

Department of Mechanical Engineering, E.G.S. Pillay Engineering College
*Department of Mechanical Engineering, S.A Engineering College

(2022년 12월 16일 접수, 2023년 5월 21일 수정, 2023년 5월 25일 채택)

Effect of Nanographene Oxide on the Mechanical Properties of EPDM/SBR Nano-composites

P. C. Prakash†, G. Gurumoorthi, V. Navaneethakrishnan, and S. Vishvanathperumal*

Department of Mechanical Engineering, E.G.S. Pillay Engineering College, Nagapattinam, Tamilnadu-611002, India
**Department of Mechanical Engineering, S.A Engineering College, Chennai, Tamilnadu-600077, India*

(Received December 16, 2022; Revised May 21, 2023; Accepted May 25, 2023)

Abstract: The curing (optimum cure (t_{90}) and scorch time (t_{s2}), cure rate index (CRI), torque difference (ΔM), maximum torque (M_h) and minimum torque (M_l)), physical (hardness, rebound resilience, compression set and abrasion resistance), and mechanical properties (tensile strength, tensile modulus, tear strength and elongation at break) of ethylene-propylene-diene monomer terpolymer (EPDM)/styrene-butadiene copolymer rubber (SBR) nano-composites with additions of modified nano-graphene oxide (mGO) for possible usage as flexible and durable materials were examined in this study. Nano-graphene oxide (GO) was treated with two types of surfactants, 3-aminopropyltriethoxysilane (KH550) coupling agent and 4,4'-diphenylmethane diisocyanate (MDI), and then incorporated into an EPDM/SBR rubber matrix at a varying loading (2-10 phr), mixed by an open mill mixer, and vulcanized by hydraulic press. The particle size altered after modification, and the modified GO diffused efficiently in the EPDM/SBR rubber matrix, according to the FESEM. The MDI modified GO nano-composites have better mechanical properties than the KH550 modified GO nano-composites. The findings suggest that the produced nano-composites could be employed in a diversity of outdoor uses, including window seals, door seals and cooling system hoses.

Keywords: ethylene-propylene-diene monomer terpolymer/styrene-butadiene copolymer rubber, graphene oxide, modifier, mechanical properties.

Introduction

Nano-fillers have the potential to indirectly modify the mechanical and physical characteristics of the polymer matrix in nano-composites.[1-2] A brand-new class of materials called nano-composites[3-4] has at least one dimension that is on the nanoscale. Nano-composites can be divided into three groups based on the filler geometries. Fumed SiO_2, and powder of nano-metallic materials have 3D in the range of nanometer,[5-6] whiskers and carbon nanotubes (CNTs) have 2D in the range of nanometer,[7-8] and mica, and clay, have ID in the range of nanometer.[9-11] In fact, activators and crosslinking agents can be efficiently adsorb by nano-fillers, boosting the matrix cross-linking density in the vicinity of the nano-fillers.[12] Due to their distinctive properties, rubber-like substances have been employed in a wide range of applications, including shoes, pipelines, seals, and tyres. These industrial objectives, as well as the exceptional advancement of nano-fillers and nano-scale characterization tools, have led to an intense focus on the mechanical properties of rubber compounds filled with nanoparticle fillers in recent years (see, for example, References[13-19]).

SiO_2 and carbon black (CB) are frequently used as key reinforcing fillers in the tyre industry.[20-23] In comparison to traditional micro-composites, layered silicate loaded nano-composites have significantly better mechanical, thermal, and barrier properties.[24-26] A fascinating substance with potential uses as a rein-

†To whom correspondence should be addressed.
pcprakash.tpt@gmail.com, ORCID 0000-0002-8700-8624

forcing ingredient for polymer nanocomposites, graphene has recently gained a great deal of attention.[27-28] With a planar sheet of sp^2 linked carbon atoms that is one atom thick and tightly packed in a honeycomb crystal structure, graphene is regarded as two-dimensional carbon nanofiller.[29] Outstanding physical characteristics of defect-free graphene include its high heat conductivity (5000 W/m K), Young's modulus (1 TPa), and ultimate tensile strength of 130 GPa. Additionally, graphene has a large specific area, high electron mobility, and gas permeability. As a result, it might be a viable candidate for a nanofiller to improve the mechanical, electrical, and thermal qualities of composite materials. Several methods, including as chemical vapour deposition (CVD) of methane gas,[30] one-step graphite exfoliation,[31] and graphite oxide thermal reduction,[32] have been utilised to create graphene.

Graphene oxide (GO) is a good choice for the formulation of rubber composite in a diversity of applications due to its hydrophilic nature and low rate. The existence of polar functional groups on the surface of GO, for instance hydroxyl, carboxylic, and epoxy, allows for interactions with a variety of polar matrixes.[33-40] The properties of GO nano-filler and the efficiency of the resulting composite are significantly influenced by the type and processing of the graphite utilised. Therefore, GOs nano-filler with different levels of oxidation are quite interesting, especially in the production of composite materials. Various ways have been used to vary the degree of GO oxidation,[41-47] such as adjusting the acid combination,[48] reaction/oxidation duration,[49] oxidant levels,[44] and so on. One of the most efficient methods is to synthesise GO using microscopic graphite as a precursor. Deemer *et al.*[47] examined the oxygen functional assemblies of GO generated by Hummer's and Mercano-Tour's methods. The particle size of graphite has a significant impact on the amount of oxygen functional assemblies in GO, according to the study.

Several scholars have examined the influence of graphene oxide modification on polymer characteristics in recent decades. In order to improve the nanocomposites' electrical conductivity and gas barrier, Kim *et al.*[50] modified GO with phenyl isocyanate before incorporating it with polyurethane (PU). GO was used by Deshmukh *et al.*[51] to improve the thermal and mechanical properties of polyvinyl chloride (PVC). To improve the thermal stability of nanocomposites, Wang *et al.*[52] produced silicone rubber (SR)/GO nanocomposites. Functionalized graphene sheets (FGSs) are used by Ozbas *et al.*[53] to increase the mechanical characteristics, electrical conductivity and gas permeability of SR (type: PDMS i.e., poldimethysiloxane). Electrical percolation was detected in composite materials with a conductivity of 0.8 wt% FGS. Gan *et al.*[54] used graphene nanoribbon to improve the physical, mechanical and thermal properties of SR nanocomposites. Shao *et al.*[55] altered graphene oxide by taking advantage of the hydrogen bonds formed between the oxygen groups of the GO surface (GO) and the hydroxyl groups in cellulose. According to Xu *et al.*[56] the tensile strength and thermal conductivity of SR composites modified with 3-aminopropyltriethoxysilane coupling agent (KH550) increased by 33 and 56%, respectively, while similar compounds modified with 4,4-diphenylmethane diisocyanate (MDI) increased by 50 and 31%. Furthermore, The particle shape of GO changed following modification, and TEM images showed that MDI-modified GO had a better dispersion morphology.

However, comprehensive study on the impact of modified nanographene oxide (mGO) on the cure behaviour, mechanical characteristics, and morphology of ethylene-propylene-diene monomer terpolymer (EPDM)/styrene-butadiene copolymer rubber (SBR), particularly in terms of abrasion resistance, is lacking. In most cases, EPDM/SBR compound is employed in outdoor applications. Surface modification of GO with 4,4′-diphenylmethane diisocyanate (MDI) and 3-aminopropyltriethoxysilane coupling agent (KH550) is used to increase GO dispersion in EPDM/SBR rubber mixtures. The modified GO is then mixed with an EPDM/SBR rubber mixture to create modified GO-EPDM/SBR nano-composites. The maximum filler loading of 10 phr was chosen since composites at this level are practically agglomerated. The infuence of nano-particles on the composites' cure parameters, tensile and tear properties, and morphology is studied. Following that, the influence of altered GO on the characteristics of composites is mostly investigated by destructive testing.

Experimental

Materials. SBR copolymer (Grade: 1502, Emulsion type, content of styrene - 23.4%, Mooney viscosity (ML1+4 @ 100 ℃) - 51 MU, density at 20 ℃ - 0.94 g/cm^3, decomposition temp > 200 ℃, flash point > 300 ℃, organic acids - 6 wt%, ash content - 0.1 weight %, volatile matter - 0.2 weight %, soaps - 0.2 weight %) was procured from Relflex Elastomers Stretching Limits, Chennai, India. Ethylene-propylene-diene monomer (EPDM Grade: S 512 F, ethylene content - 69%, termonomer content (ethylidene norbornene) - 4.5%, Mooney viscosity (ML1+4 @ 125 ℃) - 63 MU) was procured from Dalmia Polymers LLP Private Limited, New Delhi, India. Graphite flake, with a

carbon basis of 99%, ≈325 mesh particle size (≥ 99%), molecular weight - 12.01 g/mol, was purchased from Sigma-Aldrich Chemical Pvt. Ltd., Puducherry, India. Dibutyltin dilaurate (DBTDL), *N*,*N*-dimethylacetamide (DMAc), 4,4′-diphenylmethane diisocyanate (MDI), KH550, dichloromethane, $NaNO_3$, H_2SO_4, $KMnO_4$, H_2O_2, HCl, xylene, mesitylene, benzene, toluene, n-heptane, n-octane, n-pentane, n-hexane, carbon tetrachloride and chloroform were also purchased from Sigma-Aldrich Chemical Pvt. Ltd., Puducherry, India. Stearic acid, zinc oxide, mercapto-benzo-thiazyl di-sulphide (MBTS), sulphur and tetramethyl-thiuram di-sulphide (TMTD) of merck grade were gotten from Vignesh Chemicals Pvt. Ltd., Chennai, India.

Preparation of Graphene Oxide (GO). First, graphene oxide (GO) was produced using the modified Hummers technique.[57] At 0 ℃, 10 g graphite flake (30-50 μm), 7.5 g $NaNO_3$, and 460 mL H_2SO_4 were combined. Within 1 hour, 30 g $KMnO_4$ was progressively introduced into the concoction, followed by 2 hours of stirring in an ice-water bath. 1000 mL of 10-weight percent H_2SO_4 was accompanying in 1 hour after additional stirring at ambient temperature for five days. At 98 ℃, the resulting mixture was agitated for another 2 hours. The temperature was then reduced to 60 ℃, and 30 mL of dilute H_2O_2 were added. After being agitated for two hours at ambient temperature, the mixture was precipitated, then cleaned several times with an aqueous solution of 6-weight percent H_2SO_4/1-weight percent H_2O_2 and filtered. The resulting solid was then rinsed three times with a 6-weight percent and 1.2-weight percent HCl solution. GO was then filtered and dried for a week in a vacuum oven after being rinsed with deionized water until the pH was nearly 7.[58-59]

Preparation of GO Modified by Isocyanate (MDI-GO). GO was dried using a vacuum oven at 80 ℃ for three hours. To create a homogenous dispersion, GO was ultrasonicated in anhydrous N,N-dimethylacetamide (DMAc). Under nitrogen, the aforementioned mixture was stirred while being heated to 80 ℃. A few drops of DBTDL were added to the dispersion after MDI (4,4-diphenylmethane diisocyanate) was dissolved in anhydrous DMAc. The reaction was kept at 80 ℃ for four hours. The mixture was centrifuged and repeatedly washed with acetone to remove any leftover MDI after cooling to ambient temperature. In a vacuum oven set at 50 ℃ for 24 hours, the homogeneous product was dried.[56]

Preparation of GO Modified by KH550 (KH550-GO). GO was dried using a vacuum oven at 80 ℃ for three hours. Then, 400 mg of GO were added to anhydrous ethanol and ultrasonically processed for 20 minutes to create a homogeneous dispersion. After that, 4 g of KH550 saturated in anhydrous ethanol was ultrasonically agitated for 30 minutes with the dispersion. The mixture was mixed and cooked for 24 hours at 80 ℃. After cooling, the mixture was centrifuged and repeatedly washed with anhydrous ethanol to get rid of any residual KH550. The finished product was dried in a vacuum oven for 24 hours at 60 ℃.[56]

Preparation of GO-EPDM/SBR Nanocomposites. On an open mill mixer, mGO fillers and EPDM/SBR gum were mixed together to make mGO-EPDM/SBR composites. The following is the compounding formula: EPDM is 80 phr, SBR is 20 phr, mGO is variable (0, 2, 4, 6, 8, and 10 phr), sulphur is 2.5 phr, ZnO is 5 phr, stearic acid is 2 phr, MBTS is 1 phr, and TMTD is 1 phr. The compounds were then hydraulically pressed for the optimum cure time (t_{c90}) at 160 ℃ under 60 MPa. The composites have a sheet thickness of about 2 mm. Finally, for mechanical testing, the composites were cut into ASTM standard specimens.

Characterization. The nanocomposites were cured for optimum cure time (90%) at 160 ℃ with 3° arc in the Monsanto Rheometer R-100 testing apparatus (standard: ASTM D-2084). The following eq. (1) was used to construct the cure rate index (CRI).

$$\text{Cure rate index, CRI } (\text{min}^{-1}) = \frac{100}{t_{C90} - t_{S2}} \quad (1)$$

where, t_{S2} - scorch time, t_{c90} - cure time. Scorch time (t_{s2}) (min): This is the amount of time needed to generate 2% of the maximum torque (M_H). Optimum Cure Time (t_{90}) (min): This is the amount of time needed to reach 90% of the M_H.

The tensile properties were determined using standard: ASTM D-412-C. The EPDM/SBR-mGO composites' tensile properties (stress at 100% elongation (100% modulus), elongation at break, and tensile strength) were tested at 23 ℃ using a UTM equipment (Dak System Inc.), with a gauge length of 33 mm and an extension rate of 500 $\text{mm}\cdot\text{min}^{-1}$. At least four test samples were used to evaluate tensile characteristics, and the average result was determined and reported. Using ASTM D-624-C, the tear strength was ascertained. The surface morphology was studied using SEM (S-4200, Hitachi, Tokyo, Japan).

The hardness of the material was done using a Shore-A durometer according to ASTM-D-2240. It was calculated in five distinct locations on the specimens, with the median value being given. Using a rebound tester (Resiliometer), the rebound resilience was assessed according to ASTM D-2632. The DIN abrasion tester (Zwick Abrasion tester, model 6102) was used

to ascertained the abrasion resistance of vulcanised rubber compound, as required by ASTM Standard ASTM D-5963. The morphological characteristics of EPDM/SBR nanocomposites were studied using micro-photomicrographs acquired with a SEM (ZEISS EVO 18 MA's SEM). The samples first received a gold sputter coating. The following eq. (2) can beused to calculate the abrasion loss:

$$\text{Abrasion loss } (\text{mm}^3) = \frac{\Delta m \times S_0}{\rho \times S} \quad (2)$$

where, Δm - mass loss in mg, ρ - density in mg/mm^3, S_0 - nominal abrasive power (value: 200 in mg, constant), S - average abrasive power in mg.

Results and Discussion

Cure Characteristics. Where the product is to be moulded, the curing characteristics of the polymer or elastomer are critical. Cure properties such as torques (M_h, minimum torque (M_l), and delta torque (ΔM)), timings (t_{s2} and t_{90}), and CRI can be used to measure the processability of EPDM/SBR nanocomposites. For EPDM/SBR nanocomposites containing varying concentrations of GO and mGO (MDI-GO and KH550-GO), the cure time for curing compounds was evaluated, as well as changes in cure time for different loadings (GO, MDI-GO and KH550-GO).

M_l, which varies in direct relation to the viscosity of the rubber compounds, is the torque at the beginning of vulcanization. Figure 1 demonstrations the M_l of EPDM/SBR nanocomposites loaded with various concentrations of GO, MDI-GO, and KH550-GO. With loadings of GO at 10 phr, MDI-GO, and KH550-GO up to 8 phr and 6 phr, respectively, the minimum torque rise. The minimum torque then decreased with increasing loading, however it was lower in nanocomposites containing GO than in those loaded with MDI-GO and KH550-GO. Because torque is proportional to stiffness, the results showed that increasing the quantity of MDI-GO and KH550-GO in the rubber matrix enhances vulcanizate stiffness.[60-62]

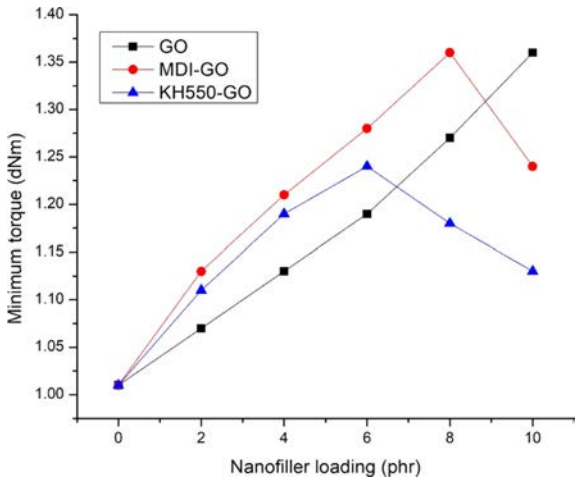

Figure 1. The M_l of EPDM/SBR composites with modified GO.

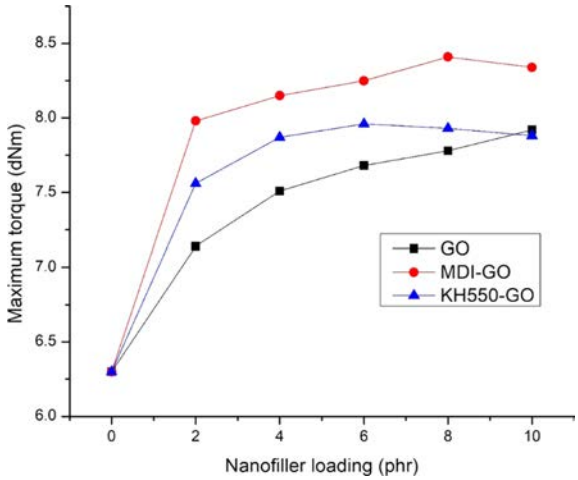

Figure 2. The M_h of EPDM/SBR composites with modified GO.

The maximum torque indicates the fully vulcanised rubber's shear modulus at the vulcanization temperature, which increases with filler loading.[62] Figure 2 shows the M_h of EPDM/SBR nanocomposites loaded with various concentrations of GO, MDI-GO, and KH550-GO. The maximum torque increases as the GO loading in the nanocomposite increases, although in the case of nanocomposites loaded with MDI-GO and KH550-GO, the maximum torque increased up to 8 phr and 6 phr, respectively, before declining. This enhance was a subsidiary indication for better inter-facial adhesion between mGO and EPDM/SBR rubber matrix. Upon a further incorporation of GO and cluster of the nano-filler in the EPDM/SBR rubber matrix, this elucidation confirmed that the addition of MDI-GO and KH550-GO in EPDM/SBR rubber affects the processability of the rubber nanocomposite and hence both the KH550-GO and MDI-GO can operate as a reinforcement agent for the EPDM/SBR rubber matrix.

Figures 3 and 4 show the changes in scorch and cure times as a function of GO content in EPDM/SBR nanocomposites, respectively. The inclusion of GO reduces both scorch and cure times, however the t_{s2} and t_{90} for EPDM/SBR nanocomposites loaded with modified-GO reduced up to 8 phr and 6 phr for MDI-GO and KH550-GO, respectively, before increasing. This decrease is because of a stronger interaction between GO and

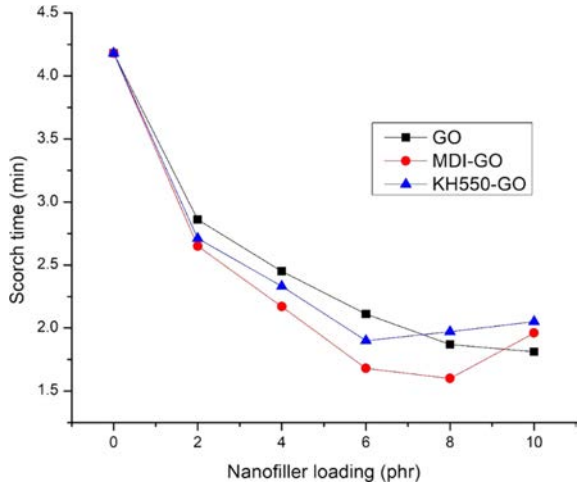

Figure 3. The t_{s2} of EPDM/SBR composites with modified GO.

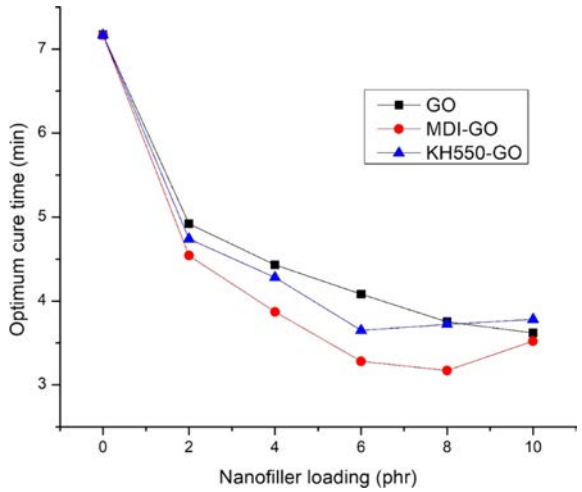

Figure 4. The t_{90} of EPDM/SBR composites with modified GO.

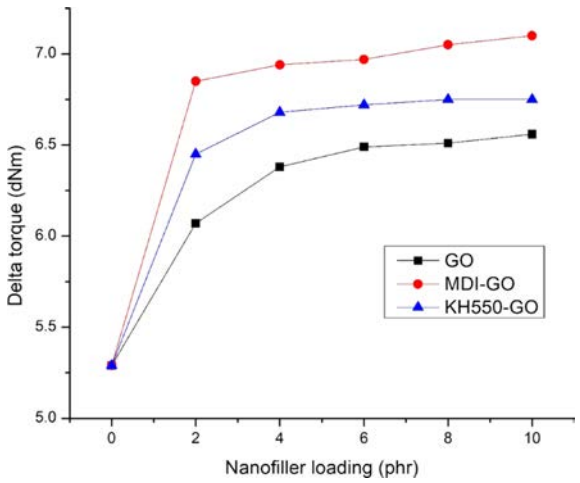

Figure 5. The ΔM of EPDM/SBR composites with modified GO.

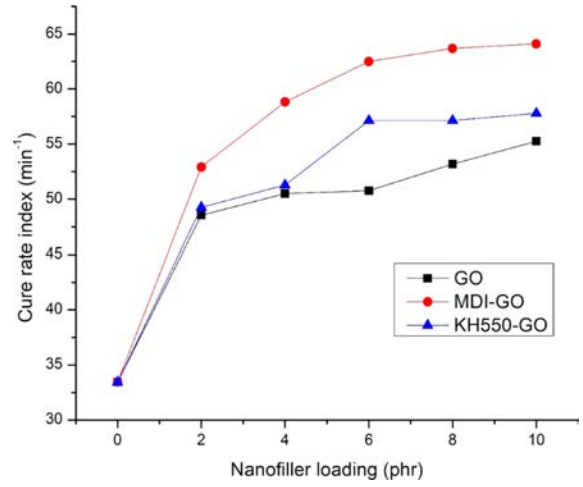

Figure 6. The CRI of EPDM/SBR composites with modified GO.

the EPDM/SBR elastomeric matrix, which is caused by the high surface area of these fine size particles, and the main reason for this decrease is because of the homogeneous distribution of GO in the EPDM/SBR elastomeric matrix. Consequently, there was an increase in productive efficiency (productivity) and a reduction in processing energy use. The increased scorch and optimum cure time for modified mGO after 8 phr and 6 phr could be attributed to mGO particle agglomeration or simply physical contact between adjacent agglomerates. In EPDM/SBR nanocomposites, the agglomeration forms a domain that acts as a foreign body. The existence of a large amount of clusters in greater mGO loadings acts as a barrier to chain movement, resulting in inferior rheometric properties.[61-62]

The delta torque and cure rate index (CRI) (rate of curing response) both showed an increased trend, as shown in Figures 5 and 6, respectively. The rise in CRI is more noticeable when using MDI modifier, which could be attributable to a significant improvement in the interfacial rubber-filler contact, which leads to improved rheometric characteristics. GO was treated with MDI to enhance distribution in the rubber blend matrix. The delta torque is clearly higher with EPDM/SBR-MDI-GO compound, especially for the EPDM/SBR-KH550-GO compound, due to the improved reinforcing efficiency. Modifier led to better GO dispersion and distribution by avoiding GO re-agglomeration after compounding. In conclusion, adding MDI-GO and KH550-GO to EPDM/SBR nanocomposites improved heat stability after vulcanization, reduced t_{s2}, increased crosslinking density or increased ΔM, and made processing easier by decreasing the reaction of vulcanization.

Tensile Properties. The tensile properties of rubber blend

(EPDM/SBR) vulcanizates at varied nanofiller (GO, MDI-GO, and KH550-GO) concentrations are shown in Figure 7(a)-(c). Tensile parameters of nanocomposites include 100% modulus, elongation at break and tensile strength. Modulus is the force at a specific elongation value, *i.e.*, 100% elongation. Expressed in megapascals (MPa), modulus is most widely used for testing and comparison purposes at 100% elongation. This is referred to as "M100" or modulus 100. There has been the development of a traditional composite since the unaltered GO nanofiller has a poor reinforcing effect. The rubber composites reinforced with MDI and KH550 modified GO, on the other hand, had stronger 100% modulus and tensile strength than the unmodified GO composites, as exposed in Figure 7(a)-(b). The nanoscale structure of the modified-GO is responsible for significant increases in tensile qualities at low concentrations of both MDI and KH550 modified-GO, as expected. The nanocomposite samples containing 8 phr MDI and KH550 modified GO had the strongest tensile strength. The improved tensile qualities point to a significant interaction between the EPDM/SBR rubber matrix and the modified-GO. The schematic diagram of GO, MDI-GO, and KH550-GO as shown in Figure 8. The schematic diagram of interaction between EPDM/SBR rubber matrix and modified GO is shown in Figure 9. GO was treated with MDI to enhance distribution in the rubber blend matrix. The distribution of nanofiller in a rubber blend matrix is one of the most important factors influencing the physical attributes of the finished goods.[63]

With the GO content increasing, the 100% modulus and tensile strength properties of rubber blend nanocomposites are improved, as represented in Figure 7(a) and (b). The 100% modulus and tensile strength of GO-rubber blend nanocomposites increase from 6.75 and 1.44 MPa to 19.54 and 2.52 MPa, respectively (≈189% and 75% increases over the base EPDM/SBR rubber matrix, respectively) when the untreated GO content increases from 0 to 6 phr. On the other hand, the 100% modulus and tensile strength of KH550-GO-rubber blend nanocomposites increase from 6.75 and 1.44 MPa to 21.56 and 3.08 MPa, respectively (≈219% and 114% increases over the base EPDM/SBR rubber matrix, respectively) when the KH550-GO content increase from 0 to 8 phr. As the MDI-GO loading increases from 0 to 8 phr, the 100% modulus and tensile strength of MDI-GO/rubber blend nanocomposites upsurge from 1.44 and 6.75 MPa to 3.29 and 23.08 MPa, respectively. The improvement in mechanical characteristics of MDI-GO is more noticeable than that of GO with the same nanofiller loading. Compared with the neat EPDM/SBR rubber blend, MDI-GO/EPDM/SBR

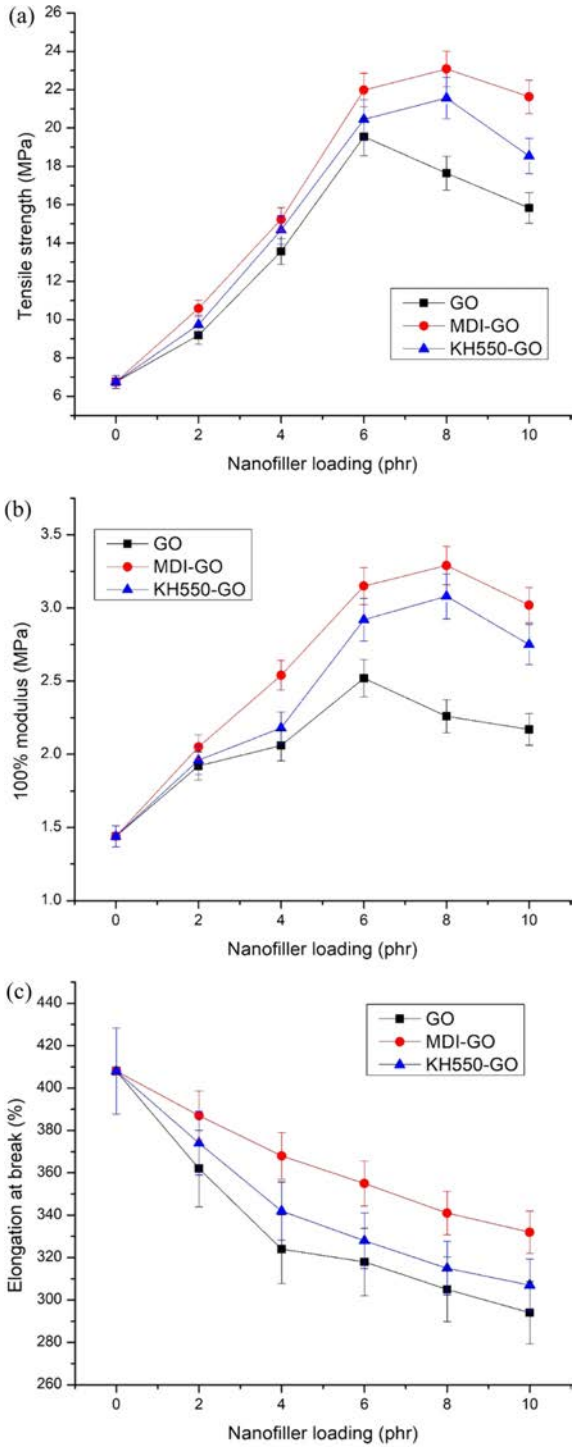

Figure 7. The effect of modified GO on the tensile properties of EPDM/SBR rubber composites: (a) tensile strength; (b) 100% modulus; (c) elongation at break.

nanocomposites with only 8 phr MDI-GO exhibit an awe-inspiring enhancement in tensile strength (≈242% upsurge over the base rubber blend), and 100% modulus (≈128% upsurge

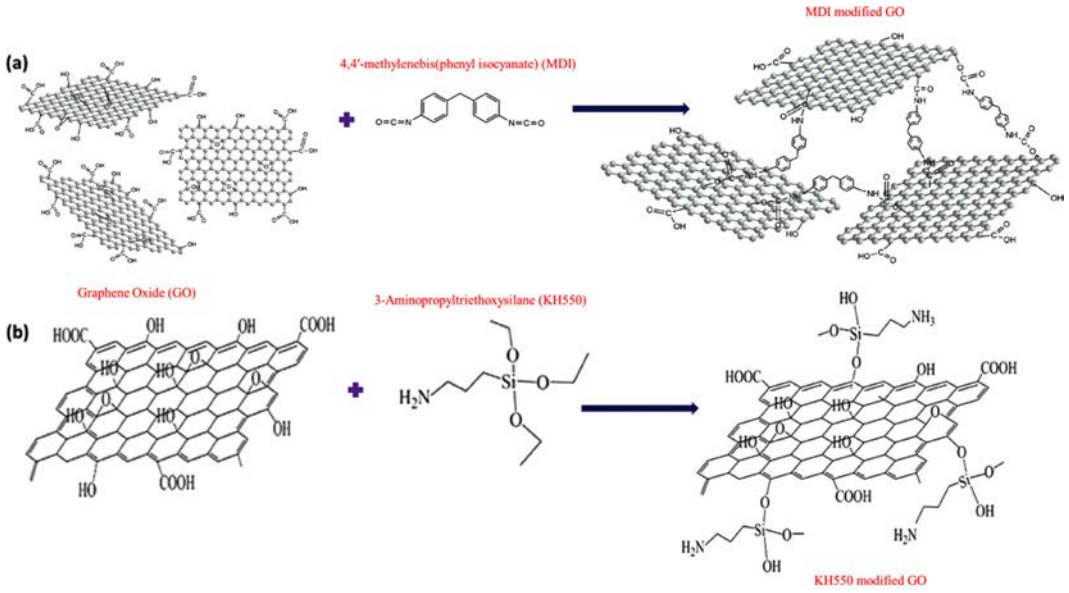

Figure 8. Schematic diagram of GO, MDI-GO and KH550.

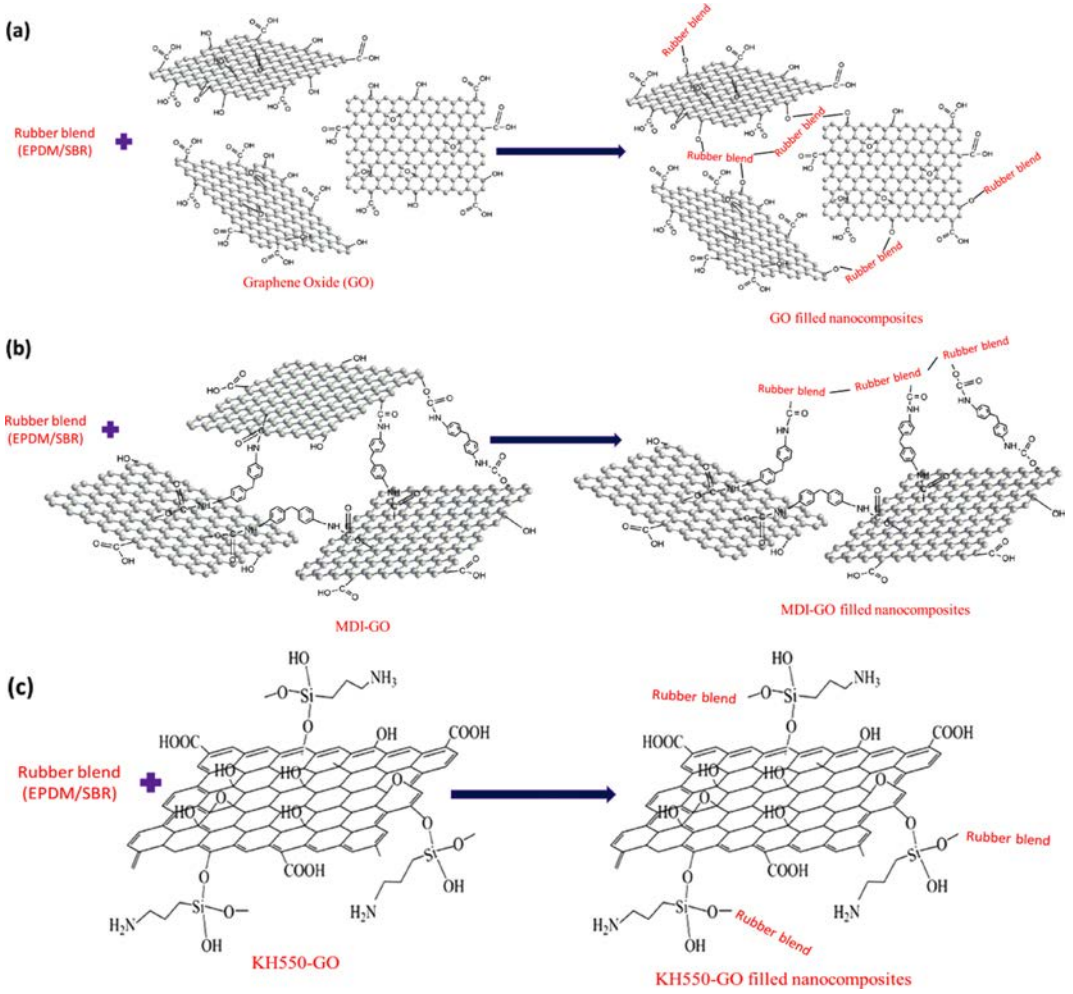

Figure 9. Schematic diagram of interaction between EPDM/SBR rubber matrix and modified GO: (a) GO filled nanocomposites; (b) MDI-GO filled nanocomposites; (c) KH550-GO filled nanocomposites.

over the base rubber blend), revealing that MDI-GO had a high-efficiency improvement to support the load transfer. This high improving efficiency may be interconnected with the well-dispersement or distribution of MDI-GO in the elastomeric matrix and strong interfaces between MDI-GO and the rubber blend matrix. The elongation at break of both unmodified GO based rubber blend and modified-GO based rubber blend nanocomposites decreases with the nanofillers loading increasing (Figure 7(c)), which may be due to low flexibility of unmodified-GO and modified-GO, as well as the poor interfaces of unmodified GO and the EPDM/SBR rubber matrix in unmodified-GO/EPDM/SBR nanocomposites. Even a minor increase in the amount of GO, up to 6 phr for untreated GO and 8 phr for mGO, will result in considerable increases in the 100% modulus and strength of the rubber blend nanocomposites loaded with untreated GO. MDI-GO filled nanocomposite > KH550 filled nanocomposite > untreated GO filled nanocomposite. This ranking is explained by a larger specific surface area and easier physical interactions between GO and polymer matrix due to the functional groups.[64-65] Quick aggregation, poor interfacial adhesion, low tensile strength, and 100% modulus are all results of GO dispersion.[60,66-68] The unavoidable aggregation of the GO at high nanofiller content can be attributed to lower tensile strengths reported for samples above 6 phr GO and 8 phr mGO loading.

Tear Strength. The tear strength of rubber blend-GO nanocomposites is shown in Figure 10. Base rubber has a tear strength of 14.21 N/mm. At 6 phr GO, the tear strength reached its greatest value, and at 10 phr, the tear strength decreased. The agglomeration is responsible for the decrease in tear strength at 10 phr. Under the applied load, the agglomerated particle is the weak spot. The agglomeration zone is more prone to see fracture initiation or propagation than the well-distributed GO zone. The results reveal that the property of 8 phr mGO filled nanocomposites is nearly constant in both the modifier. As a result of the findings, it appears that GO agglomeration is an unavoidable phenomenon in nanocomposites at higher GO concentrations, resulting in lower characteristics irrespective of modifiers, which can be improved by using other modifiers.

Hardness and Rebound Resilience. Figures 11 and 12 depict the nanocomposites' hardness and rebound resilience, respectively. The higher the filler loading, the more reinforcement effect and crosslinks are generated during vulcanization, confining the polymer chains' free ends. The hardness of the material increases as the degree of crosslinking increases. The more compact the networks are, the shorter the molecular lengths between

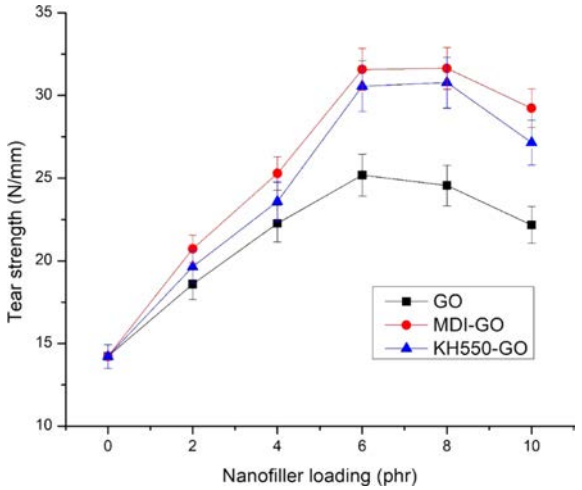

Figure 10. The effect of modified GO on the tear strength of EPDM/SBR rubber composites.

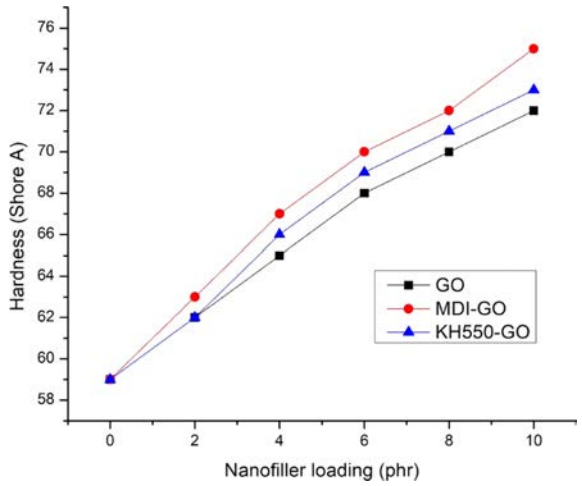

Figure 11. The effect of modified GO on the hardness of EPDM/SBR rubber composites.

crosslinks are, and so the network is tighter, resulting in increased hardness. The high hardness value is attributable to the strongly reinforcing GO's greater surface area. Modified nanofillers filled nanocomposite materials had better mechanical properties in terms of modulus, tensile strength, and hardness compared to the GO due to the inclusion of stiff filler particles. The nanofiller's reinforcing impact caused the hardness values to rise as filler loadings increased. The MDI modified GO filler had a stronger reinforcing effect in EPDM/SBR nanocomposites than the KH550 modified GO filler. Specific surface area, particle size, polymer type, and surface-activity of the filler particles have all been found to influence the reinforcing of nanocomposite materials.[69] As a result, adding nanofiller to the EPDM/SBR rubber matrix increased material hardness while lowering rebound

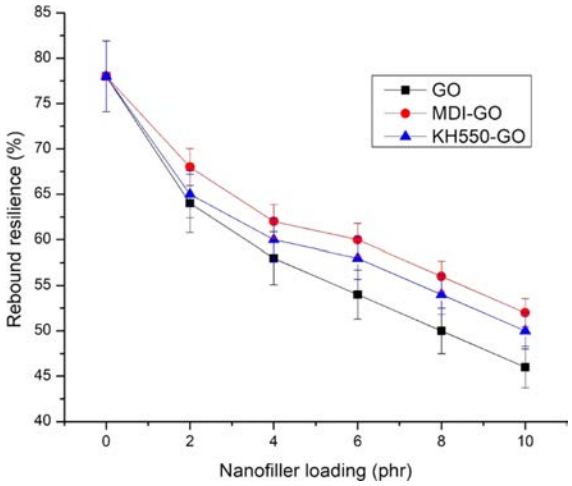

Figure 12. The effect of modified GO on the rebound resilience of EPDM/SBR rubber composites.

resilience in the resulting GO, MDI-GO, or KH550-GO filler-filled nanocomposites. In both the MDI-GO and KH550-GO nanocomposites, the rebound resilience reduced marginally as the nanofiller loadings increased. However, due to the better reinforcement capabilities of the GO, the mechanical properties of the MDI-GO filler filled EPDM/SBR nanocomposites were higher than those of the KH550-GO ones.

Abrasion Resistance. The abrasion resistance of EPDM/SBR vulcanizates was assessed using the DIN volume loss. Figure 13 depicts the volume loss of EPDM/SBR/GO, EPDM/SBR/MDI-GO, and EPDM/SBR/KH550-GO vulcanizates with varying GO levels. As the GO concentration in EPDM/SBR/GO vulcanizates increased, the volume loss of the vulcanizates decreased. Rubber abrasion is determined by its resistance to fracture or tearing when it comes into touch with sharp asperities. The use of reinforcing fillers (GO) in nanocomposites improves abrasion resistance by preventing the polymer matrix from breaking. As a result, a higher concentration of GO was more effective at preventing rubber matrix tearing. However, at a concentration of 10 phr, introducing GO to EPDM/SBR nanocomposites only decreased DIN volume loss from 79.1 to 46.4 mm^3. For all MDI-GO contents, a notable reduction in the DIN volume loss of EPDM/SBR compounds was attained in the case of EPDM/SBR/MDI-GO nanocomposites. For unfilled blends and nanocomposites containing MDI-GO 2, 4, 6, 8, and 10 phr, the DIN volume loss of EPDM/SBR/MDI-GO decreased from 79.1 to 54.3, 50.5, 48.2, 46.5, and 45.1 mm^3, respectively. According to FESEM pictures of their surfaces of tensile fracture specimens and hardness data, which will be discussed later, MDI-GO has a better dispersion and distribution in the EPDM/SBR than EPDM/SBR/GO and EPDM/SBR/KH550-GO nanocomposites. Since MDI-GO nanofillers have a greater surface area than KH550-GO and unmodified GO, this increased the interaction between MDI-GO and EPDM/SBR. Vishvanathperumal *et al.*[17] reported outcomes that were comparable. They found that when an EPDM/SBR rubber matrix was slid against a smooth steel counterface, the wear resistance of the EPDM/SBR rubber was enhanced by a homogeneous distribution of nanoclay. At an MDI-GO loading of 10 phr, all EPDM/SBR nanocomposites had the lowest DIN volume loss. This was assumed to be due to MDI-GO agglomeration at increasing concentrations, as evidenced in FESEM micrographs in Figure 12 where agglomeration increased as the amount of MDI-GO increased. Aside from the above mentioned reasons, it was discovered that adding MDI-GO to the rubber matrix increased hardness, which could aid to improve abrasion resistance. Vishvanathperumal *et al.*[18] reported similar findings. They discovered that higher hardness of nanocomposites corresponded to enhanced abrasion resistance of nanosilica filler filled EPDM/SBR.

Morphology of Composites. To explore the interfacial quality in the polymer composites, the tensile fracture surface of the samples was observed by FESEM after a tensile test. Rubber nanocomposites' huge specific surface area, strong van der Waals force between the GO, and increased rubber matrix viscosity all contribute to GO's facile agglomeration. GO must therefore be evenly distributed throughout the polymer matrix in order to produce high-performance nanocomposites. In the GO/EPDM/SBR composites, a thick sheet structure is observed on the matrix surface (Figure 14(a)), and the GO aggregations can be seen at the edge of the sheet structure. In the GO/EPDM/

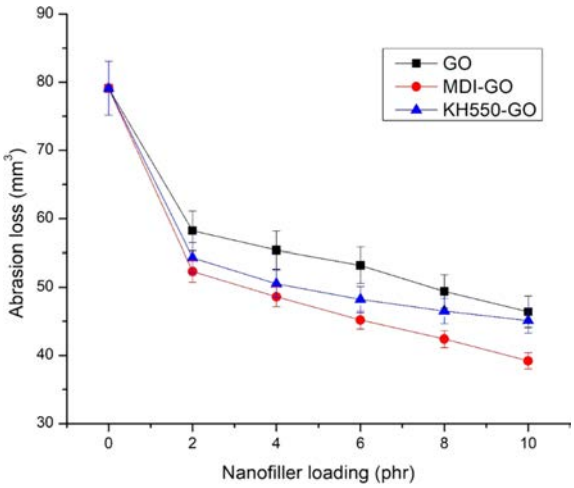

Figure 13. The effect of modified GO on the abrasion loss of EPDM/SBR rubber composites.

SBR composites, the same GO aggregates also can be noticed (Figure 14(a)), and some obvious gaps are observed, confirming no interaction between the GO sheets and polymer matrix. During the failure process, the aggregates and the gaps could induce some micro-cracks to fail the strength of composites. Figure 14 (b) and (c) illustrates the morphology of the cracked surface for the EPDM/SBR rubber nanocomposites with KH550-GO and MDI-GO (8 phr). As seen in Figure 14(c), MDI-GO organizes itself row by row in a regular fashion in the EPDM/SBR nanocomposites. It is possible to see through rigorous interface monitoring that modified GO was distributed uniformly in EPDM/SBR nanocomposites and solidly coupled with the rubber matrix. Due to the unconnected aggregation structure of GO, MDI-GO disperses more effectively than KH550-GO (Figure 12(b)). In the case of MDI-GO/EPDM/SBR composites, no obvious clusters of MDI-GO sheets are noticed. The image of MDI-GO/EPDM/SBR composites in Figure 14(c) reveals that a relatively good compatibility of MDI-GO and the polymer matrix is obtained, and no sheet/matrix gaps are observed on the fracture surface, indicating the improvement of interfacial interaction between MDI-GO and EPDM/SBR matrix after surface functionalization. Furthermore, the contact area of MDI-GO and EPDM/SBR matrix is smooth (Figure 14(c)), and some polymer molecules seem to be grafted on the surface of MDI-GO sheet. This interaction can promote the local stress transfer between the polymer matrix and sheets efficiently to improve the strength of composites.[70-71]

Crosslinking Density. The cross-link density of the nanocomposites was calculated using swelling value measurements and the Flory–Rehner equation.[72-73]

$$M_c = \frac{-\rho_p V_s V_r^{1/3}}{\ln(1-V_r)+V_r+\chi V_r^2} \quad (3)$$

$$V_r = \frac{1}{1+Q_m} \quad (4)$$

$$v = \frac{1}{2M_c} \quad (5)$$

where, M_c denotes the molar mass of the polymer between crosslinks, ρ_p denotes the density of the polymer, V_s denotes the molar volume of the toluene, V_r denotes the volume fraction of elastomer in the solvent-swollen filled compound, χ denotes the interaction parameter of the polymer (0.3),[74] Q_m denotes the weight swell of the rubber nanocomposites with nanofiller in solvent and v denotes the degree of crosslink density.

The mechanical characteristics of the vulcanizates will be directly impacted by the change in crosslink density. The cross-link density of the GO-filled EPDM/SBR nanocomposite rises from 2 to 10 phr, according to the findings (Figure 15). The cross-link densities of the nanocomposites filled with GO, MDI-GO, and KH550-GO provide as evidence for this. With an increase in GO content, the cross-link density also increases. It might be connected to an increase in nanofiller particles in the matrix of EPDM and SBR. When the rubber's molecular mobility decreases, toluene has a harder time penetrating the

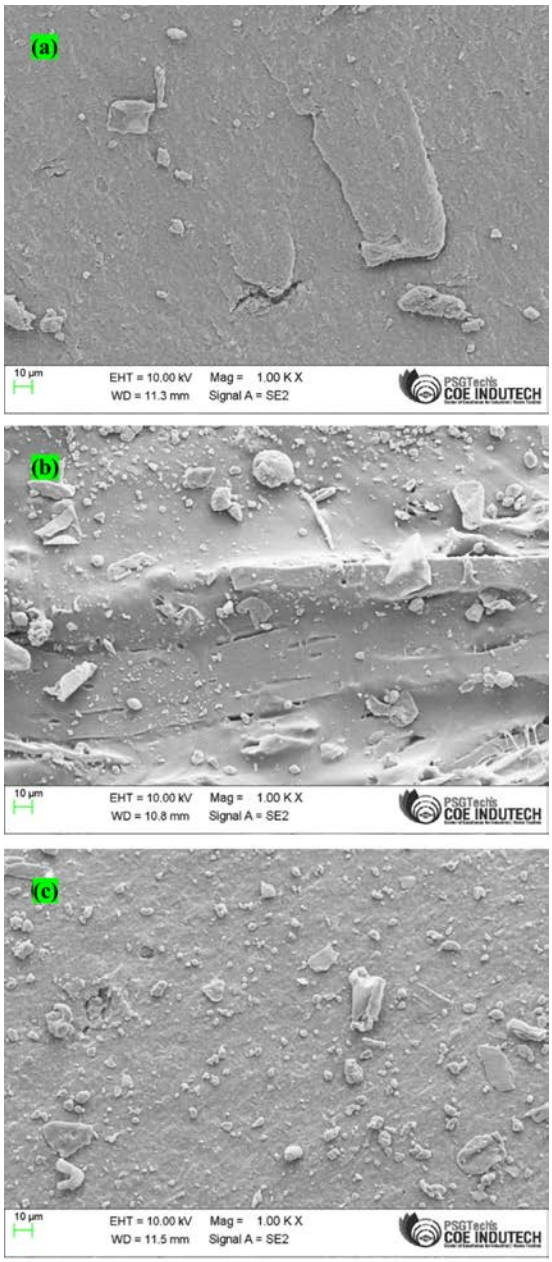

Figure 14. FESEM images of (a) unmodified GO; (b) KH550 modified GO; (c) MDI modified GO at a nanofiller content of 8 phr in the EPDM/SBR rubber matrix.

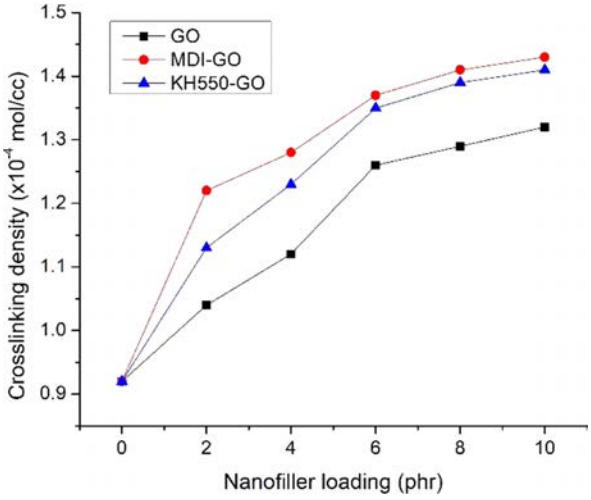

Figure 15. Crosslinking density of EPDM/SBR-GO nanocomposites.

rubber matrix. EPDM/SBR nanocomposites with MDI-GO nanofiller outperformed those with KH550-GO or GO in terms of cross-link density. The crosslinking density of the EPDM/SBR nanocomposites rose along with the amount of nanofiller. By increasing crosslinking density, tear strength, hardness, tensile strength, and abrasion resistance are all enhanced.

Conclusions

This article analyzed the effects of modified GO on the cure and mechanical properties of EPDM/SBR rubber nanocomposites. The findings demonstrated that the two GO modification strategies had different effects on nanocomposites' characteristics. The dispersion morphology of MDI modified GO was better, as demonstrated in the FESEM images. The cure parameters of the nanocomposites were still good at low loadings with the addition of modified GO (8 phr for MDI-GO and 6 phr for KH550-GO). On the other hand, the introduction of modifier in GO broke the network structure of graphene nanofiller. As a result, the addition of modified GO significantly decreased the scorch time and optimum cure time of the nanocomposites. Furthermore, nanocomposites synthesized from GO modified with MDI showed significant torques (minimum, maximum, and delta torque). Nanocomposites produced with MDI modified GO enhanced their tensile strength and abrasion resistance by 242% and 50%, respectively, while nanocomposites developed with KH550 modified GO increased by 219% and 43%, respectively. These findings suggested that incorporating graphene to EPDM/SBR rubber could be a promising way to prepare outdoor materials.

References

1. Krishnan, V. N.; Kumar, C. S.; Ganesan, G. Investigation of Wear Behavior of Hybrid Polymer Nanocompsoite. *Mater. Res. Express* **2018**, 5, 085302.
2. Krishnan, V. N.; Kumar, C. S.; Ganesan, G. Evaluation of Tensile Properties of Epoxy Nanocomposite. *J. Adv. Microscopy Res.* **2018**, 13, 166-170.
3. Navaneethakrishnan, V.; Senthilkumar, C.; Ganesan, G. Wear Behavior of An Epoxy/HNT Composite. *Mater. Testing* **2017**, 59, 1061-1066.
4. Krishnan, V. N.; Kumar, C. S.; Ganesan, G. Evaluation of Tribological Properties of Epoxy Nanocomposite. *J. Adv. Microscopy Res.* **2017**, 12, 110-115.
5. Jana, S. C.; Jain, S. Dispersion of Nanofillers in High Performance Polymers Using Reactive Solvents as Processing Aids. *Polymer* **2001**, 42, 6897-905.
6. Saujanya, C.; Radhakrishnan, S. Structure Development and Crystallization Behavior of PP/nanoparticulate Composite. *Polymer* **2001**, 42, 6723-6731.
7. Calvert, P. Potential Applications of Nanotubes. In: Ebbesen TW, Editor. Carbon Nanotubes. Boca Raton, FL: CRC Press; 1997.
8. Favier, V.; Canova, G. R.; Shrivastava, S. C.; Cavaille, J. Y. Mechanical Percolation in Cellulose Whisker Nanocomposites. *Polym. Eng. Sci.* **1997**, 37, 1732-1739.
9. Theng, B. K. G. The Chemistry of Clay-organic Reactions. New York: Wiley; 1974.
10. Chen, G. H.; Wu, D. J.; Weng, W. G.; Yan, W. L. Preparation of Polymer/graphite Conducting Nanocomposites by a Intercalation Polymerization. *J. Appl. Polym. Sci.* **2001**, 82, 2506-2513.
11. Pan, Y. X.; Yu, Z. Z.; Ou, Y. C.; Hu, G. H. A New Process of Fabricating Electrically Conducting Nylon 6/graphite Nanocomposites Via Intercalation Polymerization. *J. Polym. Sci. Part B: Polym. Phys.* **2000**, 38, 1626-1633.
12. Wolff, S. Chemical Aspects of Rubber Reinforcement by Fillers. *Rubber Chem. Tech.* **1996**, 69, 325-345.
13. Vishvanathperumal, S.; Gopalakannan, S. Effects of the Nanoclay and Crosslinking Systems on the Mechanical Properties of Ethylene-propylene-diene Monomer/styrene Butadiene Rubber Blends Nanocomposite. *Silicon* **2019**, 11, 117-135.
14. Vishvanathperumal, S.; Gopalakannan, S. Swelling Properties, Compression Set Behavior and Abrasion Resistance of Ethylene-propylene-diene Rubber/styrene Butadiene Rubber Blend Nanocomposites. *Polymer Korea* **2017**, 41, 433-442.
15. Vishvanathperumal, S.; Anand, G. Effect of Nanoclay/Nanosilica on the Mechanical Properties, Abrasion and Swelling Resistance of EPDM/SBR Composites. *Silicon* **2020**, 12, 1925-1941.
16. Vishvanathperumal, S.; Navaneethakrishnan, V.; Gopalakannan S. The Effect of Nanoclay and Hybrid Filler on Curing Characteristics, Mechanical Properties and Swelling Resistance of Ethylene-vinyl Acetate/styrene Butadiene Rubber Blend Composite. *J. Adv. Microscopy Res.* **2018**, 13, 469-476.
17. Vishvanathperumal, S.; Anand, G. Effect of Nanosilica and

Crosslinking System on the Mechanical Properties and Swelling Resistance of EPDM/SBR Nanocomposites with and Without TESPT. *Silicon* **2021**, 13, 3473-3497.
18. Vishvanathperumal, S.; Anand, G. Effect of Nanosilica on the Mechanical Properties, Compression Set, Morphology, Abrasion and Swelling Resistance of Sulphur Cured EPDM/SBR Composites. *Silicon* **2022**, 14, 3523-3534.
19. Ganeche, P. S.; Balasubramanian, P.; Vishvanathperumal, S. Halloysite Nanotubes (HNTs)-Filled Ethylene-Propylene-Diene Monomer/Styrene-Butadiene Rubber (EPDM/SBR) Composites: Mechanical, Swelling, and Morphological Properties. *Silicon* **2022**, 14, 6611-6620.
20. Mei, H.; Zhang, C.; Wang, R.; Feng, J.; Zhang, T. Impedance Characteristics of Surface Pressure-sensitive Carbon Black/silicone Rubber Composites, *Sensor. Actuat A Phys* **2015**, 233, 118-124.
21. Song, Y.; Yu, J.; Dai, D.; Song, L.; Jiang, N. Effect of Silica Particles Modified by In-situ and Ex-situ Methods on the Reinforcement of Silicone Rubber, *Mater. Design* **2014**, 64, 687-693.
22. Senthilvel, K.; Vishvanathperumal, S.; Prabu, B.; John Baruch, L. Studies on the Morphology, Cure Characteristics and Mechanical Properties of Acrylonitrile Butadiene Rubber with Hybrid Filler (carbon black/silica) Composite. *Polym. Polym. Compos.* **2016**, 24, 473-480.
23. Vishvanathperumal, S.; Gopalakannan, S. Reinforcement of Ethylene Vinyl Acetate with Carbon Black/silica Hybrid Filler Composites. *Appl. Mechanics Mater.* **2016**, 852, 16-22.
24. Kojima, Y.; Usuki, A.; Kawasami, M. Mechanical Properties of Nylon-6-clay Hybrid. *J. Mater. Res.* **1993**, 6, 1185-1189.
25. Lagaly, G. Introduction: from Clay Mineral-polymer Interactions to Clay Mineral-polymer Nanocomposites. *Appl. Clay. Sci.* **1999**, 15, 1-9.
26. Vishvanathperumal, S.; Navaneethakrishnan, V.; Anand, G.; Gopalakannan, S. Evaluation of Crosslink Density Using Material Constants of Ethylene-Propylene-Diene Monomer/Styrene-Butadiene Rubber with Different Nanoclay Loading: Finite Element Analysis-Simulation and Experimental. *Adv. Sci. Eng. Medicine* **2020**, 12, 632-642.
27. Kim, H.; Abdala, A. A.; Macosko, C. W. Graphene/polymer nanocomposites. Macromolecules **2010**, 43, 6515-6530.
28. Zheng, D.; Tang, G.; Zhang, H.-B.; Yu, Z.-Z.; Yavari, F.; Koratkar, N. Lim, S.-H.; Lee, M.-W. In Situ Thermal Reduction of Graphene Oxide for High Electrical Conductivity and Low Percolation Threshold in Polyamide 6 Nanocomposites. *Compos. Sci. Technol.* **2012**, 72, 284-289.
29. Kuilla, T.; Bhadra, S.; Yao, D.; Kim, N. H.; Bose, S.; Lee, J. H. Recent Advances in Graphene Based Polymer Composites. *Prog. Polym. Sci.* **2010**, 35, 1350-1375.
30. Kim, K. S.; Zhao, Y.; Jang, H.; Lee, S. Y.; Kim, J. M.; Kim, K. S. Ahn, J.-H.; Kim, P.; Choi, J.-Y.; Hong, B. H. Large-scale Pattern Growth of Graphene Films for Stretchable Transparent Electrodes. *Nature* **2009**, 457, 706-710.
31. Lee, J. H.; Shin, D. W.; Makotchenko, V. G.; Nazarov, A. S.; Fedorov, V. E.; Kim, Y. H. Choi, J.-Y.; Kim, J. M.; Yoo, J.-B. One-step Exfoliation Synthesis of Easily Soluble Graphite and Transparent Conducting Graphene Sheets. *Adv. Mater.* **2009**, 21, 4383-4387.
32. Schniepp, H. C.; Li, J. L.; McAllister, M. J.; Sai, H.; Herrera-Alonso, M.; Adamson, D. H.; Prud'homme, R. K.; Car, R.; Saville, D. A.; Aksay, I. A. Functionalized Single Graphene Sheets Derived from Splitting Graphite Oxide. *J. Phys. Chem. B* **2006**, 110, 8535-8539.
33. Moghaddam, S. Z.; Sabury, S.; Sharif, F. Dispersion of rGO in Polymeric Matrices by Thermodynamically Favorable Self-assembly of GO at Oil–water Interfaces. *RSC Adv.* **2014**, 4, 8711.
34. Pierleoni, D.; Xia, Z. Y.; Christian, M.; Ligi, S.; Minelli, M.; Morandi, V.; Doghieri, F.; Palermo, V. Graphene-based Coatings on Polymer Films for Gas Barrier Applications. *Carbon N. Y.* **2016**, 96, 503-512.
35. Zhang, P.; Xu, P.; Fan, H.; Sun, Z.; Wen, J. Covalently Functionalized Graphene Towards Molecular-level Dispersed Waterborne Polyurethane Nanocomposite with Balanced Comprehensive Performance. *Appl. Surf. Sci*. **2019**, 471, 595-606.
36. Yuan, N. Y.; Ma, F. F.; Fan, Y.; Liu, Y. B.; Ding, J. N. High Conductive Ethylene Vinyl Acetate Composites Filled with Reduced Graphene Oxide and Polyaniline. Compos. *Part A Appl. Sci. Manuf*. **2012**, 43, 2183-2188.
37. Wu, W.; Wan, C.; Zhang, Y. Graphene Oxide as a Covalent-crosslinking Agent for EVMg-PA6 Thermoplastic Elastomeric Nanocomposites, *RSC Adv.* **2015**, 5, 39042-39051.
38. She, X.; He, C.; Peng, Z.; Kong, L. Molecular-level Dispersion of Graphene Into Epoxidized Natural Rubber: Morphology, Interfacial Interaction and Mechanical Reinforcement. *Polymer* **2014**, 55, 6803-6810.
39. Huang, Y.; Qin, Y.; Zhou, Y.; Niu, H.; Yu, Z. Z.; Dong, J. Y. Polypropylene/graphene Oxide Nanocomposites Prepared by In Situ Ziegler-natta Polymerization. *Chem. Mater*. **2010**, 22, 4096-4102.
40. Kotal, M.; Banerjee, S. S.; Bhowmick, A. K. Functionalized Graphene with Polymer as Unique Strategy in Tailoring the Properties of Bromobutyl Rubber Nanocomposites. *Polymer* **2016**, 82, 121-132.
41. Emiru, T. F.; Ayele, D. W. Controlled Synthesis, Characterization and Reduction of Graphene Oxide: A Convenient Method for Large Scale Production. *Egypt. J. Basic Appl. Sci*. **2017**, 4, 74-79.
42. Yuan, R.; Yuan, J.; Wu, Y.; Chen, L.; Zhou, H.; Chen, J. Efficient Synthesis of Graphene Oxide and the Mechanisms of Oxidation and Exfoliation. *Appl. Surf. Sci*. **2017**, 416, 868-877.
43. Kumar, H. V.; Woltornist, S. J.; Adamson, D. H. Fractionation and Characterization of Graphene Oxide by Oxidation Extent Through Emulsion Stabilization, *Carbon N. Y.* **2016**, 98, 491-495.
44. Castaldo, R.; Lama, G. C.; Aprea, P.; Gentile, G.; Lavorgna, M.; Ambrogi, V.; Cerruti, P. Effect of the Oxidation Degree on Self-assembly, Adsorption and Barrier Properties of Nano-graphene. *Microporous Mesoporous Mater*. **2018**, 260, 102-115.
45. Hanifah, M. F. R.; Jaafar, J.; Othman, M. H. D.; Ismail, A. F.; Rahman, M. A.; Yusof, N.; Salleh, W. N. W.; Aziz, F. Facile Synthesis of Highly Favorable Graphene Oxide: Effect of Oxidation Degree on the Structural, Morphological, Thermal and Electrochemical Properties. *Materialia*. **2019**, 6, 100344.

46. Chen, J.; Zhang, Y.; Zhang, M.; Yao, B.; Li, Y.; Huang, L.; Li, C.; Shi, G. Water-enhanced Oxidation of Graphite to Graphene Oxide with Controlled Species of Oxygenated Groups. *Chem. Sci*. **2016**, 7, 1874-1881.
47. Deemer, E. M.; Paul, P. K.; Manciu, F. S.; Botez, C. E.; Hodges, D. R.; Landis, Z.; Akter, T.; Castro, E.; Chianelli, R. R. Consequence of Oxidation Method on Graphene Oxide Produced with Different Size Graphite Precursors. *Mater. Sci. Eng. B.* **2017**, 224, 150-157.
48. Chen, J.; Chi, F.; Huang, L.; Zhang, M.; Yao, B.; Li, Y.; Li, C.; Shi, G. Synthesis of Graphene Oxide Sheets with Controlled Sizes from Sieved Graphite Flakes. *Carbon* **2016**, 110, 34-40.
49. Guerrero-Contreras, J.; Caballero-Briones, F. Graphene Oxide Powders with Different Oxidation Degree, Prepared by Synthesis Variations of the Hummers Method. *Mater. Chem. Phys*. **2015**, 153, 209-220.
50. Kim, H.; Miura, Y.; Macosko, C. W. Graphene/Polyurethane Nanocomposites for Improved Gas Barrier and Electrical Conductivity. *Chem. Mater.* **2010**, 22, 3441-3450.
51. Deshmukh, K.; Joshi, G. M. Thermo-mechanical Properties of Poly(vinyl chloride)/graphene Oxide as High Performance Nanocomposites. *Polym. Test*. **2014**, 34, 211-219.
52. Wang, X.; Dou, W. Preparation of Graphite Oxide (GO) and the Thermal Stability of Silicone Rubber/GO Nanocomposites. *Thermochim. Acta* **2012**, 529, 25-28.
53. Ozbas, B.; O'Neill, C. D.; Register, R. A.; Aksay, I. A.; Prud'homme, R. K.; Adamson, D. H. Multifunctional Elastomer Nanocomposites with Functionalized Graphene Single Sheets. *J. Polym. Sci. Pol. Phys*. **2012**, 50, 910-916.
54. Gan, L.; Shang, S. M.; Yuen, C. W. M.; Jiang, S. X.; Luo, N. M. Facile Preparation of Graphene Nanoribbon Filled Silicone Rubber Nanocomposite with Improved Thermal and Mechanical Properties. *Compos. Part B* **2015**, 69, 237-242.
55. Shao, W.; Liu, H.; Liu, X.; Wang, S.; Zhang, R. Anti-bacterial Performances and Biocompatibility of Bacterial Cellulose/graphene Oxide Composites. *Rsc. Advances* **2015**, 5, 4795-4803.
56. Yan, X.; Qun, G.; Hongqin, L.; Kangsheng, Z. Effects of Functional Graphene Oxide on the Properties of Phenyl Silicone Rubber Composites. *Polym. Testing* **2016**, 54, 168-175.
57. Becerril, H. A.; Mao, J.; Liu, Z.; Stoltenberg, R. M.; Bao, Z.; Chen, Y. ACS Nano 2 463-70 Paredes JI, Villar-Rodil S, Martınez-Alonso A and Tascón JMD 2008. *Langmuir* **2008**, 24, 10560-10564.
58. Bai, J.; Liao, X.; Huang, E.; Luo, Y.; Yang, Q.; Li, G. Control of the Cell Structure of Microcellular Silicone Rubber/nanographite Foam for Enhanced Mechanical Performance. *Mater. Des.* **2016**, 133, 288-298.
59. Gan, L.; Shang, S.; Marcus Yuen, C. W.; Jiang, S.-X. Impact of Vinyl Concentration of a Silicone Rubber on the Properties of the Graphene Oxide Filled Silicone Rubber Composites. *Composites Part B* **2015**, 84, 294-300.
60. Song, S. H.; Jeong, H. K.; Kang, Y. G. Preparation and Characterization of Exfoliated Graphite and Its Styrene Butadiene Rubber Nanocomposites. *J. Ind. Eng. Chem.* **2010**, 16, 1059-1065.
61. Yang, J.; Tian, M.; Jia, Q. X.; Zhang, L. Q.; Li, X. L. Influence of Graphite Particle Size and Shape on the Properties of NBR. *J. Appl. Polym. Sci.* **2006**, 102, 4007-4015.
62. Yang, J.; Tian, M.; Jia, Q. X.; Shi, J. H.; Zhang, L. Q.; Lim, S. H.; Yu, Z. Z.; Mai, Y. W. Improved Mechanical and Functional Properties of Elastomer/graphite Nanocomposites Prepared by Latex Compounding. *Acta Materialia* **2007**, 55, 6372-6382.
63. Wang, L. L.; Zhang, L. Q.; Tian, M. Mechanical and Tribological Properties of Acrylonitrile–butadiene Rubber Filled with Graphite and Carbon Black. *Mater. Des.* **2012**, 39, 450-457.
64. Dhanasekar, S.; Baskar, S.; Vishvanathperumal, S. Halloysite Nanotubes Effect on Cure and Mechanical Properties of EPDM/NBR Nanocomposites. *J. Inorg. Org. Polym. Mater*. **2023**, DOI: 10.1007/s10904-023-02754-1.
65. Ragupathy, K.; Prabaharan, G.; Pragadish, N.; Vishvanathperumal, S. Effect of Silica Nanoparticles and Modified Silica Nanoparticles on the Mechanical and Swelling Properties of EPDM/SBR Blend Nanocomposites. *Silicon* **2023**, DOI: 10.1007/s12633-023-02497-1.
66. Das, R. K.; Ragupathy, K.; Kumar, T. S.; Vishvanathperumal, S. Effect of Halloysite Nanotubes (HNTs) on Mechanical Properties of EPDM/NBR Blend-Nanocomposites. *Polym. Korea* **2023**, 47, 221-232.
67. Sundar, R.; Mohan, S. K.; Vishvanathperumal, S. Effect of Surface Modified Halloysite Nanotubes (mHNTs) on the Mechanical Properties and Swelling Resistance of EPDM/NBR Nanocomposites. *Polym. Korea* **2022**, 46, 728-743.
68. Wang, L.; Zhang, L.; Tian, M. Effect of Expanded Graphite (EG) Dispersion on the Mechanical and Tribological Properties of Nitrile Rubber/EG Composites. *Wear* **2012**, 276, 85-93.
69. Jovanović, S.; Samaržija-Jovanović, S.; Marković, G.; Jovanović, V.; Adamović, T.; Marinović-Cincović, M. Mechanical Properties and Thermal Aging Behaviour of Polyisoprene/polybutadiene/styrene-butadiene Rubber Ternary Blend Reinforced with Carbon Black. *Composites Part B*. **2016**, 98, 126-133.
70. Li, Z.; Wang, R.; Young, R. J.; Deng, L.; Yang, F.; Hao, L.; Jiao, W.; Liu, W. Control of the Functionality of Graphene Oxide for Its Application in Epoxy Nanocomposites. *Polymer* **2013**, 54, 6437-6446.
71. Jiang, T.; Kuila, T.; Kim, N. H.; Ku, B. C.; Lee, J. H. Enhanced Mechanical Properties of Silanized Silica Nanoparticle Attached Graphene Oxide/epoxy Composites. *Composites Sci. Technol.* **2013**, 79, 115-125.
72. Flory, P. J.; Rehner, J. Statistical Mechanics of Crosslinked Polymer Networks. II. Swelling. *J. Chem. Phys.* **1943**, 11, 512-520.
73. Aprem, S.; Joseph, K.; Thomas, S. Studies on Double Networks in Natural Rubber Vulcanizates. *J. Appl. Polym. Sci*. **2004**, 91, 1068-1078.
74. Naseri, A. S. Z.; Jalali-Arani, A. A Comparison Between the Effects of Gamma Radiation and Sulfur Cure System on the Microstructure and Crosslink Network of (styrene butadiene rubber/ethylene propylene diene monomer) Blends in Presence of Nanoclay. *Radiat Phys. Chem.* **2015**, 115, 68-74.